Steel and Composite Structures, *Vol. 25, No. 1 (2017) 19-34*
DOI: https://doi.org/10.12989/scs.2017.25.1.019

Mechanics based force-deformation curve of steel beam to column moment joints

Arnav A. Kasar *[1], S.D. Bharti [1], M.K. Shrimali [1] and Rupen Goswami [2]

[1] *Department of Civil Engineering, Malaviya National Institute of Technology Jaipur, Jaipur-302017, India*
[2] *Department of Civil Engineering, Indian Institute of Technology Madras, Chennai-600036, India*

(*Received March 27, 2017, Revised May 31, 2017, Accepted June 02, 2017*)

Abstract. The widespread damage to steel Moment Resisting Frames (MRFs) in past major earthquakes have underscored the need to understand the nonlinear inelastic behaviour of such systems. To assess the seismic performance of steel MRF, it is essential to model the nonlinear force-deformation behaviour of beam to column joints. To determine the extent of inelasticity in a beam to column joint, nonlinear finite element analysis is generally carried out, which is computationally involved and demanding. In order to obviate the need of such elaborate analyses, a simplistic method to predict the force-deformation behaviour is required. In this study, a simple, mechanics driven, hand calculation method is proposed to obtain the force-deformation behaviour of strong axis beam to column moment joints. The force-deformation behaviour for twenty-five interior and exterior beam to column joints, having column to beam strength ratios ranging from 1.2 to 10.99 and 2.4 to 22, respectively, have been obtained. The force-deformation behaviour predicted using the proposed method is compared with the results of finite element analyses. The results show that the proposed method predicts the force-deformation behaviour fairly accurately, with much lesser computational effort. Further the proposed method has been used to conduct Nonlinear Dynamic Time History Analyses of two benchmark frames; close correspondence of results obtained with published results establishes the usefulness and computational accuracy of the method.

Keywords: moment resisting frames; column to beam strength ratio; joint panel zone; force-deformation behaviour

1. Introduction

The performance of steel Moment Resisting Frame (MRF) buildings during the 1994 Northridge and 1995 Kobe earthquakes underlined the vulnerability of moment joints. Many low and medium rise steel MRF buildings sustained structural damage in the beam to column joints. These buildings were designed and detailed according to the prevalent specifications - intended to ensure ductile performance (Krawinkler and Popov 1982). The analyses of the steel MRF buildings damaged during past earthquakes showed that the prescribed drift limits resulted in frames with large reserve elastic strengths. The extensive damage to beam to column joints led designers and researchers to agree that the damage type is unacceptable. Arguably the good performance of steel welded beam to column joints during some experiments (Popov and Pinkney 1969, Fielding and Huang 1971, Popov 1988, Popov *et al*. 1989, Xue *et al*. 1996, Zekioglu *et al*. 1997, Engelhardt and Sabol 1998) led to a belief that the welds at the beam to column interface were adequate to transfer the loads to the column corresponding to the beam capacity.

A Steel Moment Resistant Frame, when subjected to strong earthquake shaking, is expected to dissipate the seismic input energy through inelastic action without collapse. The inelasticity in different components of steel MRF - Beam-ends, Joint Panel Zone and Column ends - of beam to column joints is inevitable under strong earthquake ground shaking. Fig. 1 shows interior and exteriors moment joints of an MRF and force resultants under lateral loading.

Traditionally, to limit inelastic action at desirable locations, that is, beam ends, a minimum value of column to beam strength ration (CBSR) is prescribed. The criterion is known as strong column weak beam (SCWB) design approach. The SCWB design criterion is aimed to achieve a higher level of energy dissipation in a structural system

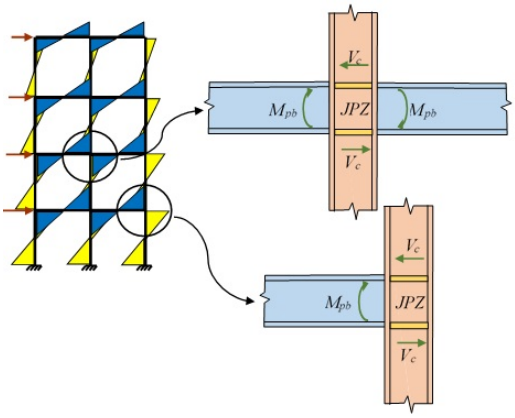

Fig. 1 Interior and Exterior Beam Column Joints in a MRF with the forces under lateral load conditions

*Corresponding author, Research Associate,
E-mail: arnav.kasar@gmail.com

ISSN: 1229-9367 (Print), 1598-6233 (Online)

through beam hinge mechanism. ANSI/AISC 341-05 (2005) suggests the SCWB design criterion to secure the ductility capacity of the steel MRFs, it prescribes that the ratio of the sum of plastic flexural strengths of columns to the sum of plastic flexural strengths of beams, connected at a joint, should be greater than unity. The inadequacy of a single parameter prescription, namely, CBSR, to attain a desirable seismic performance of steel MRF buildings has been under investigation. Research efforts – analytical as well as experimental - have been underway to understand the inelastic behaviour of various components of steel beam to column joint (Choi *et al*. 2013, Choi and Park 2012).

Joint Panel Zone (JPZ) - web area of beam to column connection delineated by the extension of beam and column flanges through the connection, transmitting moment through a shear panel (AISC 360-10 2010) – forms an important components of beam to column joint. Its behaviour and design has received considerable attention in the past. Experiments have shown that JPZ can be the weakest element in frames, and influences the behaviour of steel MRF buildings under strong seismic shaking. Since late 1960s, a number of experimental and analytical investigations have been carried out to understand the behaviour of JPZ (Huang *et al*. 1972, Krawinkler 1978, Popov 1987). These studies suggest that, when subjected to repeated cyclic distortions, yielding of JPZ is a stable phenomenon, and can be helpful in dissipating the energy induced. It is also evident from these studies that the overall frame stiffness is greatly influenced by the stiffness of the JPZ. Excessive JPZ distortion can lead to local kinking of column, which can contribute to undesirable premature fractures at the beam-to-column interface (Popov 1988). Kinking of column also results in local buckling of the beam and column flanges near the joint region. These effects can be significantly reduced by using columns with thick flanges, which also reduces the joint distortion (Krawinkler 1978, Schneider and Amidi 1988, FEMA-355C 2000, Mele *et al*. 2001). Reinforcement of columns, along with adequate detailing, has also been recommended as an effective measure to attain desirable performance of JPZ (Lee *et al*. 2005, Jin and El-Tawil 2005).

During strong seismic shaking, the antisymmetric loading on the JPZ results in large inelasticity in the beam column joint, which reduces its overall stiffness and seismic moment capacity (Popov 1988, Dubina *et al*. 2001). JPZs can sustain large post elastic shear deformations. Experiments on interior beam to column joint subassemblages showed that the panel zone shear deformation ductility of about 30 to 40 is easily achievable (Kato 1982). The post elastic stiffness is in the range of 3-8% of the elastic stiffness. This stiffness is attributed to the resistance of the panel boundary elements, the strain-hardening of the column web in the JPZ and the resistance offered by the adjoining frame members to the large deformation of the JPZ. Even when the strength of the JPZ is less than that of the adjoining frame members, it demonstrates adequate ductility and dissipates large energy with stable hysteretic loops, and is thought to be beneficial to the frame behaviour. But, the excessive yielding of JPZ enhances its shear distortion further. This increases the storey drift, which in-turn results in more damage, greater susceptibility to P-Δ effects and large permanent offsets of building frames (Schneider *et al*. 1993). JPZs that undergo large shear distortion impose smaller plastic demands at the beam ends, the large deformations of JPZs cause high shear strains and stresses at the welds connecting the beam flange to the column, thereby making the welds more conducive to crack initiation (El-Tawil *et al*. 1999). Various models, to estimate the force deformation behaviour of JPZ, has also been proposed (Krawinkler 1978, Castro *et al*. 2008). Controlling the behaviour of JPZ, and hence of the structure through design specifications, still remains a field of active research (Choi and Park 2011, Nasrabadi *et al*. 2013, Liu *et al*. 2014, Tuna and Topkaya 2015, Pan *et al*. 2016).

In order to assess the performance of a steel MRF under strong earthquake shaking, it is essential to capture the nonlinear force-deformation behaviour of beam to column joint. To determine the extent of inelasticity in beam to column joints nonlinear finite element analysis (FEA) (ABAQUS 2011) is required. The FEA process is computationally demanding. In this study a simple mechanics based analytical method has been proposed to predict the nonlinear force-deformation behaviour of beam to column joint subassemblages. The proposed hand calculation method is computationally efficient to predict the yielding sequence and force deformation behaviour of both interior and exterior moment joints, and also predicts the drifts at which inelastic actions initiate and propagate in different components of a joint. Results obtained from the proposed method, for twenty-five strong column weak beam interior and exterior joint subassemblages, have been compared with the results of FEA to ascertain the validity and correctness. Further, the proposed method has been used to carry out Nonlinear Dynamic Time History Analysis of two benchmark moment frame buildings (Tsai and Popov 1988).

2. Proposed method

The proposed simplified hand calculation method is based on basic mechanics and is able to predict the force-deformation behaviour of strong axis beam to column joints of a steel MRF along with the sequence of different modes of yielding.

Assuming rigid and unyielding connections, in a strong column weak beam moment joint, the three possible modes of yielding (Fig. 2) are,

(i) Flexural Yielding of Beam Flanges,
(ii) Shear Yielding of Joint Panel Zone and
(iii) Formation of Plastic Hinges in Beam.

Although, the preferred order of inelastic yielding, as per capacity design, is (1) Beam Flange Yielding; (2) Beam Plastic Hinges; and (3) Panel Zone Shear Yielding, the sequence of yielding depends on relative strength of the components, and hence the yield mode having least capacity shall be the first to occur. The formation of plastic hinge in beam will be preceded by yielding of beam flanges, however, shear yielding of Joint Panel Zone is

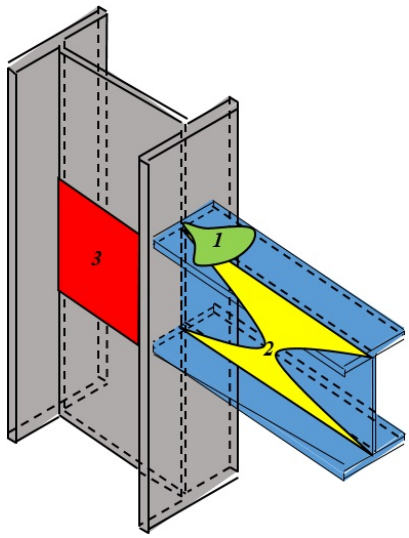

Fig. 2 A schematic of an exterior beam to column joint depicting the three probable yield locations

independent of the other two modes. The capacity of each of the components can be evaluated as follows

Beam Flange Yield Strength

$$F_{y,bf} = f_{yb} \cdot b_{bf} \cdot t_{bf} \tag{1}$$

where, f_{yb} is the yield strength of beam material, b_{bf} is width of beam flange and t_{bf} is thickness of beam flange.

Panel Zone Yield Strength

$$V_{y,pz} = \left(\frac{f_{yc}}{\sqrt{3}}\right) \cdot d_c \cdot t_{pz} \tag{2}$$

where, f_{yc} is the yield strength of column material, d_c is depth of column section and t_{pz} is the thickness of JPZ region, which is, thickness of column web (t_{cw}) and doubler plate (t_{dp}), if provided.

Beam End Force to develop Beam Plastic Hinge

$$F_{p,b} = \frac{M_{pb}}{d_b - t_{bf}} \tag{3}$$

where, M_{pb} is plastic moment carrying capacity of beam section and d_b is depth of beam section.

For beam to column moment joints the inelastic yielding of beam flanges will occur before inelastic yielding of JPZ, only when $F_{y,bf} < \frac{V_{y,pz}}{2}$ (interior joint) and $F_{y,bf} < V_{y,pz}$ (exterior joint). Further, for beam to develop plastic hinge before the yielding of JPZ is initiated, $F_{p,b} < \frac{V_{y,pz}}{2}$ (interior joint) and $F_{p,b} < V_{y,pz}$ (exterior joint).

For the known yield sequence, e.g., Panel Zone Yielding (PZY), Beam Flange Yielding (BFY), and Beam Plastic Hinging (BPH), the drift corresponding to each mode can be computed as below.

For JPZ to yield, which in this case will be the first mode of yielding, the deformation at beam end should be such that it imposes a demand of $V_{y,pz}$ in the JPZ, for which a force of $V_{y,1}$ needs to be applied at beam ends, which is given by

$$V_{y,1} = \frac{V_{y,pz}\left(d_b - t_{bf}\right)}{2 \times \left(L_b - d_c/2\right)} \tag{4}$$

where L_b is the length of beam. The resultant moment transferred to the columns due to application of force $V_{y,1}$ at beam end is

$$M_{c,1} = 2 \cdot V_{y,1} \cdot \left(\frac{L_b}{2}\right) \tag{5}$$

The rotation due to moment $M_{c,1}$ at column face is

$$\theta_{c,1} = \frac{M_{c,1}\left(L_c/2\right)}{3EI_c} \tag{6}$$

where L_c is the length of column, and E and I are properties of material and cross-section called, modulus of elasticity and moment of inertia (MoI) respectively. Also, due to application of force $V_{y,1}$ at beam ends, the JPZ of the interior joint is subjected to a force of

$$V_{pz,1} = 2 \cdot V_{y,1} \cdot \frac{\left(L_b - d_c\right)/2}{d_b - t_{bf}} \tag{7}$$

which in-turn causes a distortion.

$$\gamma_{pz,1} = \frac{V_{pz,1}}{G \cdot d_c \cdot t_{pz}} \tag{8}$$

Thus, the overall drift at beam end is obtained as the sum of drifts due to rotation of beams $\Delta_{b,1}$, rotation of columns $\Delta_{c,1}$ and rotation of JPZ $\Delta_{pz,1}$, which is obtained as

$$\Delta_{b,1} = \frac{V_{y,1}}{3EI_b}\left(\left(L_b - d_c\right)/2\right)^3 \tag{9}$$

$$\Delta_{c,1} = \theta_{c,1} \cdot \frac{L_b}{2} \tag{10}$$

$$\Delta_{pz,1} = \gamma_{pz,1} \cdot \left(L_b - d_c\right)/2 \tag{11}$$

Therefore, $\Delta_{total,1} = \Delta_{b,1} + \Delta_{c,1} + \Delta_{pz,1}$ and thus, the beam end drift at first yield is $\frac{\Delta_{total}}{L_b/2} \times 100$

For the second and third yield modes, the yield forces are to be obtained on the basis of capacity of next stronger member. The drift at which the next yield will occur can be calculated by considering post yield stiffnesses of already yielded members, in similar manner as shown above. The ultimate drift will be the beam end drift at the third yield, beyond which the joint will be completely yielded. The post yield stiffness of beam has been estimated on the basis of the reduced MoI of beam section. The stiffness of beam,

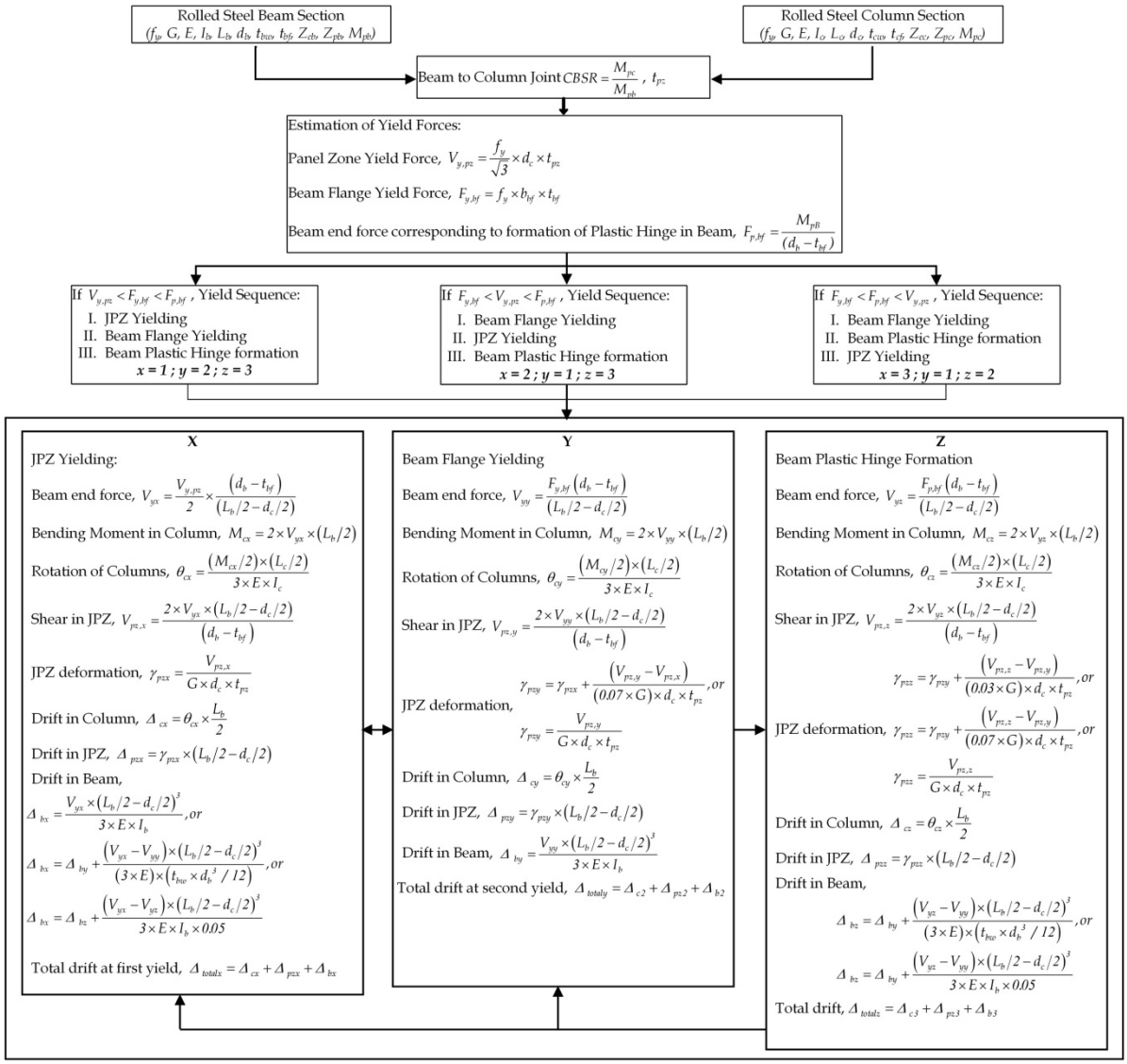

Fig. 3 Flowchart of the Proposed Method for estimation of force deformation behaviour of beam to column moment joints

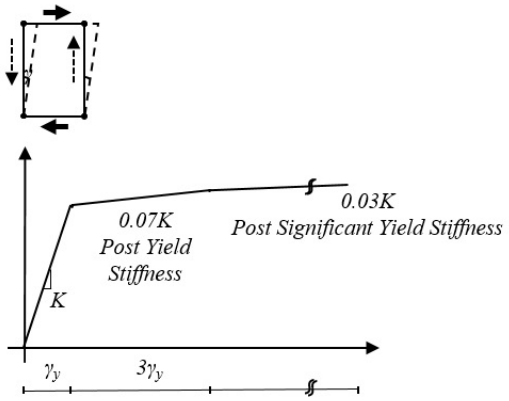

Fig. 4 Assumed force deformation behaviour of joint panel zone region

after beam flange yielding is obtained by multiplying the initial stiffness with a factor equal to the ratio of MoI of beam web and MoI of un-yielded section. Also, the post-significant yield of the beam is assumed to be 5% of its original stiffness. A flowchart for the proposed method is presented in Fig. 3.

Fig. 4 shows the force deformation behaviour of JPZ (along with the post yield stiffnesses of JPZ), adopted for the present study. Literature suggests that the post yield stiffness is approximately 7% of initial stiffness upto a rotation of $4\gamma_y$, and is 3% beyond the rotation of $4\gamma_y$ (Krawinkler 1978). This method to obtain force deformation characteristics of a strong axis beam to column joint subassemblage can be used for both interior as well as exterior joints. An illustrative example has been presented in Appendix A.

3. Validation using Finite Element Analysis

To validate the accuracy of the proposed method, finite element analyses of twenty-five exterior and interior, strong axis beam to column joint subassemblages have been carried out. The joints considered for this study are in

Table 1 List of column and beam sections used to model the subassemblages

S. No.	Column	M_{pC} (kNm)	Beam	M_{pB} (kNm)	t_{JPZ} (mm)	CBSR	
						Interior	Exterior
1.	W18×130	1,176	W27×84	986	17	1.19	2.38
2.	W21×83	787	W24×62	619	13	1.27	2.54
3.	W16×100	808	W24×62	619	15	1.31	2.62
4.	W18×130	1,176	W21×83	787	17	1.49	2.98
5.	W18×119	1,079	W21×68	636	17	1.70	3.40
6.	W14×176	1,296	W21×73	708	21	1.83	3.66
7.	W18×192	1,800	W21×93	909	24	1.98	3.96
8.	W24×176	2,078	W18×97	858	19	2.42	4.84
9.	W27×178	2,285	W21×93	909	18	2.51	5.02
10.	W24×229	2,747	W21×93	909	24	3.02	6.04
11.	W24×176	2,078	W18×71	606	19	3.43	6.86
12.	W27×235	3,148	W16×100	808	23	3.89	7.78
13.	W40×503	9,394	W18×234	2,276	39	4.13	8.26
14.	W33×318	5,157	W24×103	1,141	26	4.52	9.04
15.	W36×487	8,626	W21×166	1,779	38	4.85	9.70
16.	W27×539	7,746	W27×129	1,587	50	4.88	9.76
17.	W40×431	7,931	W18×158	1,467	34	5.41	10.82
18.	W36×529	9,484	W30×124	1,675	41	5.66	11.32
19.	W40×593	11,201	W24×162	1,914	45	5.85	11.70
20.	W36×652	11,928	W33×130	1,911	50	6.24	12.48
21.	W36×487	8,626	W27×102	1,229	38	7.02	14.04
22.	W27×539	7,746	W21×101	1,024	50	7.57	15.14
23.	W40×503	9,394	W30×90	1,114	39	8.43	16.86
24.	W36×529	9,484	W27×84	986	41	9.62	19.24
25.	W40×593	11,201	W24×94	1,019	45	10.99	21.98

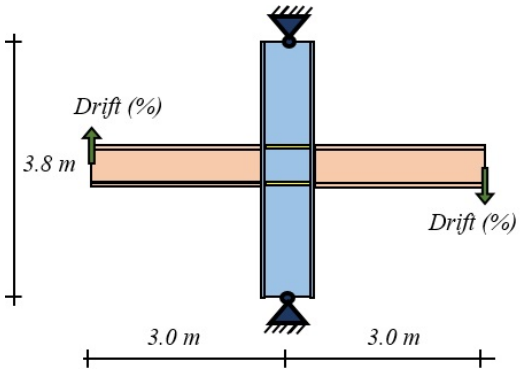

Fig. 5 Beam-column joint subassemblage

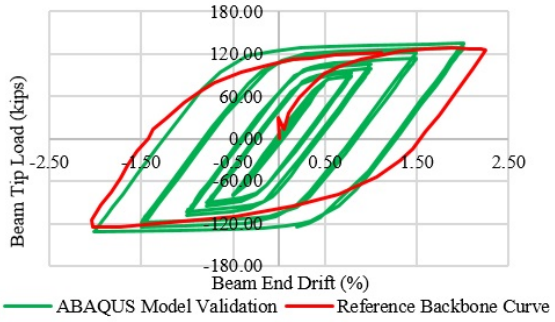

Fig. 6 Validation of the Finite Element Analysis model

compliance with the strong column weak beam design philosophy. A total of 50 beam to column joint sub-assemblages, 25 external and 25 internal are considered; selected section properties have been listed in Table 1.

The efficacy of FEA of beam to column joints has been validated by modelling an exterior beam to column moment joint, investigated experimentally by Popov 1987. The Finite Element model has been developed to simulate the experimental conditions, and the force deformation behaviour obtained analytically has been compared with the published results (Fig. 6). The close correspondence of the analysis result with experimental behaviour, establishes the adequacy of the method of analysis along with modelling and loading conditions.

The height of columns in the subassemblages is 3.8 m, which, in most cases, is the average storey height. The distance considered between column centerline and the point of application of load on beams is 3.0 m, representing a typical span. The column height is equal to the sum of

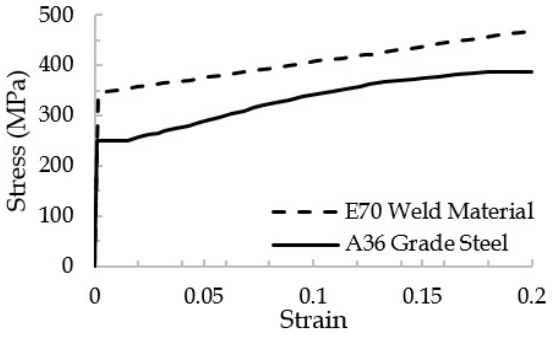

Fig. 7 Stress strain curves for A36 Steel and E70 welds as modelled

distance between points of contraflexure above and below the joint, and the beam length is taken as the distance between two points of contraflexures on either side of the column. The point of contraflexures are assumed at the mid heights of members; the subassemblage is simply supported at column ends. Centerline dimensions have been considered and displacement loading is applied at beam ends (Fig. 5). Both material and geometric nonlinearities have been considered in the analyses.

The members are of ASTM A36 grade steel with isotropic hardening model (yield stress of 250 MPa and ultimate stress of 415 MPa). Welds between beam and column of subassemblage are modelled as complete joint penetration (CJP) welds. The properties of the welds are corresponding to ASTM E70 weld electrodes, having a bilinear stress strain relationship (yield strength of 345 MPa and ultimate tensile strength of 480 MPa at 20% elongation). Stress–strain relationships for A36 Grade steel and E70 electrodes used for analysis have been shown in Fig. 7. For both the materials, modulus of elasticity and Poisson's ratio are 200 GPa and 0.30, respectively. A classically isotropic plasticity model based on von Mises yield criteria and associated plastic flow has been used to incorporate material nonlinearity.

The displacement based nonlinear finite element

Table 2 Yield locations and drifts for selected beam to column joint subassemblages obtained through Finite Element Analyses and using proposed method. The '-' indicates no inelastic action

S. No.	Exterior					Interior				
			Percentage drift at first yield					Percentage drift at first yield		
	CBSR	First yield location	Finite element analysis	Proposed method	Ratio of drift	CBSR	First yield location	Finite element analysis	Proposed method	Ratio of drift
1.	2.38	JPZ	0.75	0.68	1.10	1.19	JPZ	0.5	0.43	1.16
2.	2.54	JPZ	0.75	0.69	1.09	1.27	JPZ	0.5	0.4	1.25
3.	2.62	JPZ	0.75	0.74	1.01	1.31	JPZ	0.5	0.41	1.22
4.	2.98	JPZ	0.75	0.72	1.04	1.49	JPZ	0.5	0.4	1.25
5.	3.40	JPZ	1.00	0.91	1.10	1.70	JPZ	0.5	0.44	1.13
6.	3.66	JPZ	0.75	0.54	1.39	1.83	JPZ	-	-	-
7.	3.96	JPZ	1.00	0.94	1.06	1.98	JPZ	0.5	0.47	1.063
8.	4.84	JPZ	0.75	0.71	1.06	2.42	JPZ	0.75	0.703	1.07
9.	5.02	JPZ	0.75	0.74	1.02	2.51	JPZ	0.53	0.5	1.06
10.	6.04	JPZ	1.00	0.86	1.16	3.02	JPZ	0.75	0.75	1.00
11.	6.86	JPZ	1.00	0.80	1.25	3.43	JPZ	0.75	0.495	1.52
12.	7.78	JPZ	1.00	0.91	1.10	3.89	JPZ	0.75	0.617	1.21
13.	8.26	JPZ	2.00	1.40	1.43	4.13	JPZ	-	-	-
14.	9.04	BF	-	-	-	4.52	JPZ	1	0.755	1.32
15.	9.70	BF	-	-	-	4.85	JPZ	1	0.74	1.35
16.	9.76	JPZ	0.75	0.74	1.01	4.88	JPZ	0.75	0.495	1.51
17.	10.82	BF	1.00	0.75	1.33	5.41	JPZ	0.5	0.63	0.79
18.	11.32	JPZ	-	-	-	5.66	JPZ	1	0.46	2.17
19.	11.70	BF	1.00	0.84	1.19	5.85	JPZ	0.75	0.555	1.35
20.	12.48	BF	0.75	0.62	1.22	6.24	BF	0.75	0.725	1.03
21.	14.04	BF	-	-	-	7.02	JPZ	1	0.8	1.25
22.	15.14	BF	-	-	-	7.57	BF	1.5	0.8	1.875
23.	16.86	BF	-	-	-	8.43	BF	-	-	-
24.	19.24	BF	-	-	-	9.62	BF	-	-	-
25.	21.98	BF	-	-	-	10.99	BF	-	-	-

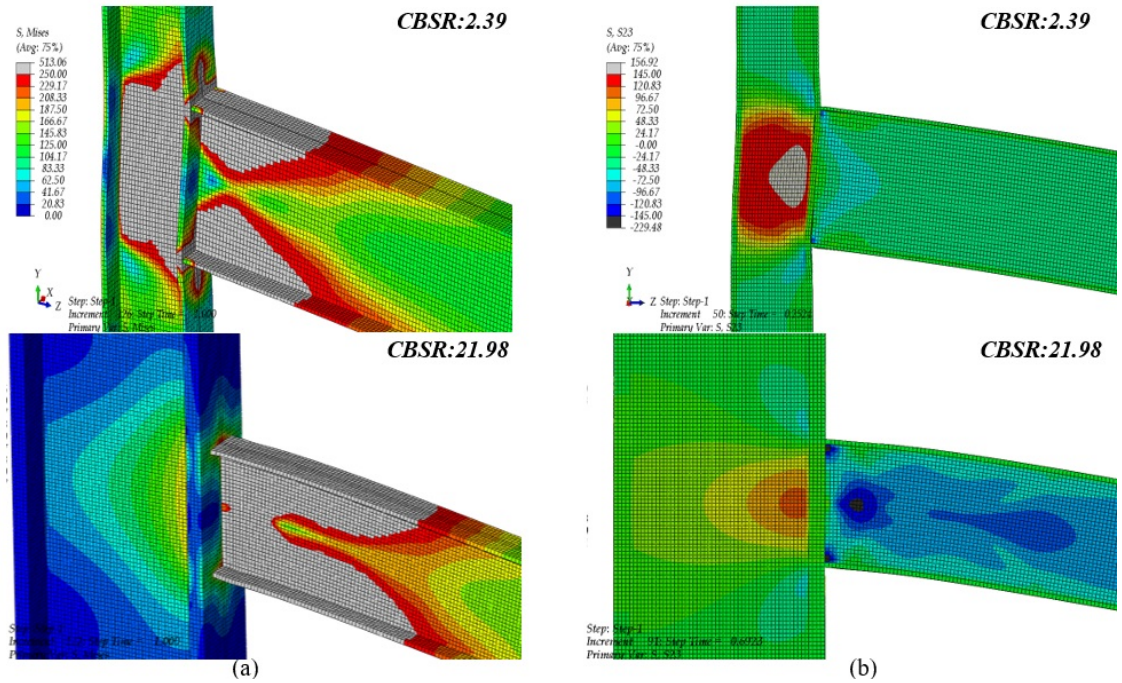

Fig. 8 (a) von Mises stress contour at 4 % drift; (b) Shear stress contours at initiation of yield

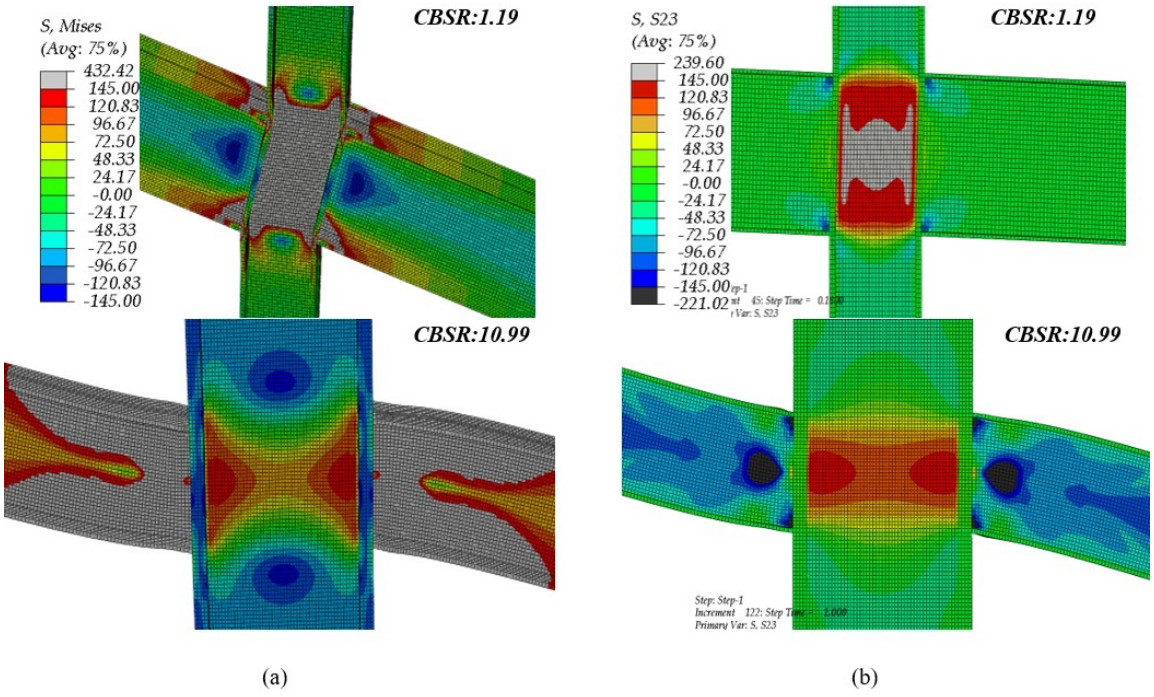

Fig. 9 (a) von Mises stress contour at 4 % drift; (b) Shear stress contours at initiation of yield

analyses, using eight noded linear brick elements (C3D8R) with uniform mesh, have been carried out using ABAQUS (2011). The CJP welds have been modelled by carefully merging the common nodes between weld elements and parent material.

The subassemblages have been subjected to single step monotonic displacements at beam ends, up to a drift of 4%, in about 125 fixed increments. The results have been presented in the form of von-Mises and shear stress contours. The reactions at the simply supported ends of the column have been monitored.

The yield drift, obtained using the proposed method, as well as from FEA, for all twenty-five beam to column joint subassemblages have been presented in Table 2. The results indicate that the percentage drift at yield, as obtained from the proposed method is in close correspondence with the yield drift observed from the FEA. It has also been observed that the minimum value of CBSR required to

prevent panel zone inelastic actions, is 7.57 and 9.04 for interior and exterior joints, respectively.

The von Mises and shear stress contours for exterior and interior beam to column joints subassemblages (for two extreme values of CBSR considered) have been shown in Figs. 8 and 9, respectively. The von-Mises stresses have been shown at 4% drift, while shear stresses have been shown at initiation of yield. Fig. 8(a) shows the von Mises stress contours for exterior joints having CBSR 2.36 and 21.98. The results indicate that for a CBSR of 2.36, the inelastic actions remain limited to the JPZ, while the beam flanges suffer limited inelastic actions. However, for a CBSR of 21.89, significant yielding of beam end region is evident, while the JPZ sustains no inelastic action. Fig. 8(b) shows the shear stress contours, which indicate that the JPZ inelasticity depends on the CBSR. The inelasticity in JPZ initiates at a drift level of 0.75% for joints having CBSR equal to 2.36. While no inelasticity is observed for joints having CBSR equal to 21.98. Fig. 9(a) shows the von Mises stress contours for interior joints having CBSR of 1.19 and 10.99. It can be observed from the stress contours that at a drift of 4%, the inelastic actions in the joint having CBSR of 1.19 remains limited to the JPZ and in the weld region due to kinking. Limited inelastic actions are also noted in

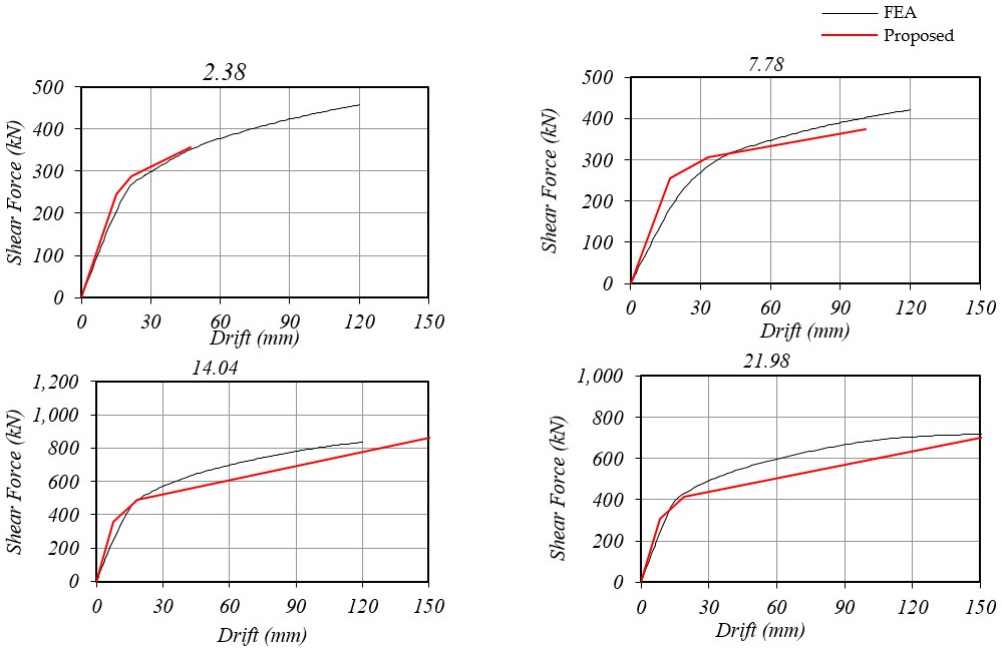

Fig. 10 Column shear force versus beam end drift relationships for exterior beam to column joints

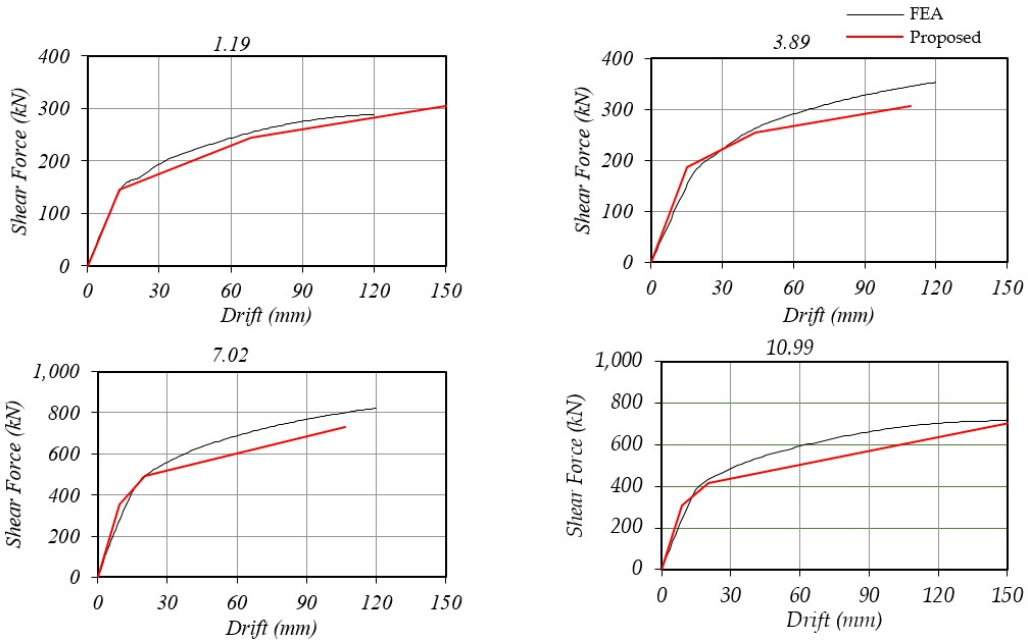

Fig. 11 Column shear force versus beam end drift relationships for interior beam to column joints

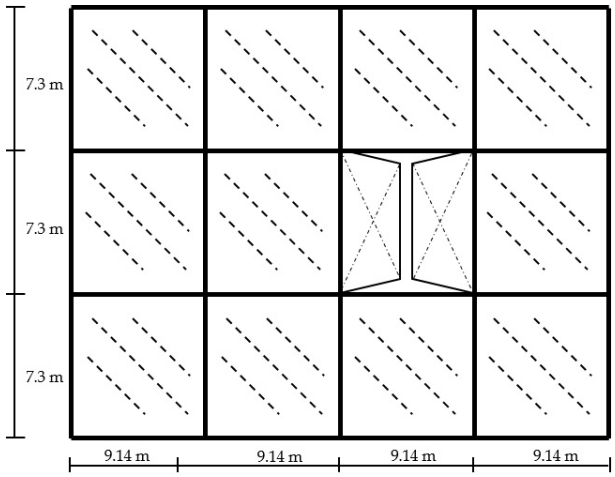

Fig. 12 Plan of six storied building frame

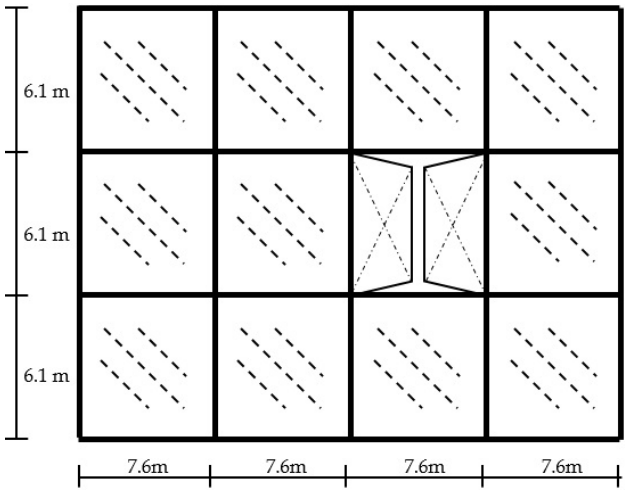

Fig. 13 Plan of twenty storied building frame

the columns, at the vicinity of the connections. However, in case of joint having CBSR of 10.99, the inelastic actions remain limited to the beams and no inelastic actions occur in the JPZ. Fig. 9(b) also suggests a similar behaviour, for joint having CBSR equal to 1.19 the inelasticity initiates in JPZ, whereas in case of joint having CBSR of 10.99, shear yielding of beam web is observed. The results of FEA analyses indicate that, minimum value of CBSR to prevent inelastic actions in JPZ, up to a drift limit of 4%, is as high as eight for both exterior and interior joints.

Figs. 10 and 11 show a comparison of proposed method and FEA in terms of force deformation relationships for exterior and interior joints, respectively. However, the proposed method predicts the force-deformation behaviour approximately, only upto the third yield level, beyond which the force deformation behaviour of the joint has not been estimated as it marks the complete yielding of joint. The apparent anomaly in the first and remaining plots of Fig. 11 is due to the fact, that in first joint, all the three assumed modes of yielding has occurred within the drift of 1.5%. The graphs indicate close correspondence between the results obtained from FEA and the proposed method, hence underscores the effectiveness of the proposed method.

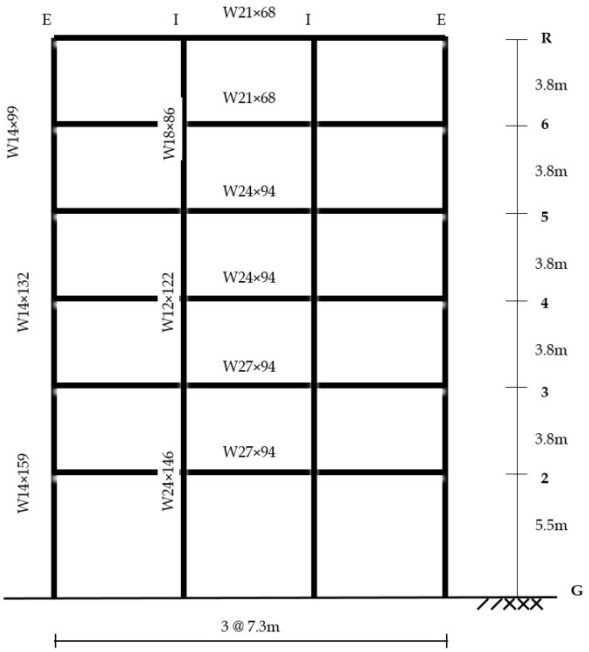

Fig. 14 Elevation of six storey benchmark frame

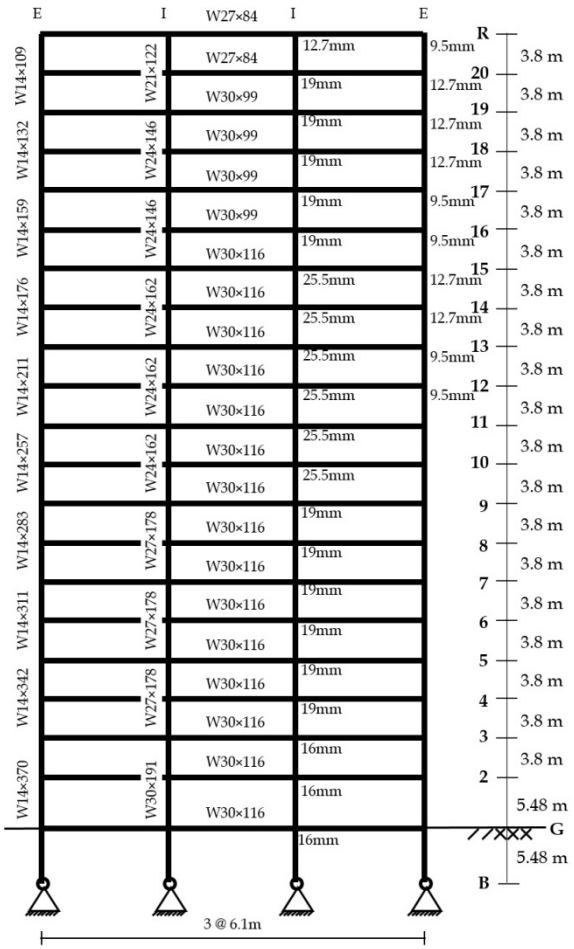

Fig. 15 Elevation of twenty storey benchmark frame

The force-deformation properties obtained using the proposed method have been used to estimate the moment-

Table 3 Proposed hinge properties for exterior and interior joints for six storey building frame

S. No.	Joint label	Yield rotation (rad)	Yield moment (kNm)	Rotation ratio (Yield/ Ultimate)	Moment ratio (Yield/ Ultimate)
1.	I2-3	0.00616	871.68	6.50	1.20
2.	I4-5	0.00608	627.53	6.58	1.53
3.	I6	0.00706	402.19	5.66	1.46
4.	E2-3	0.00803	845.13	4.98	1.34
5.	E4-5	0.00935	793.12	4.28	1.22
6.	E6	0.00898	487.25	4.46	1.32
7.	IR	0.00580	224.22	6.90	2.62
8.	ER	0.00705	341.36	5.67	1.69

Table 4 Proposed hinge property definitions for exterior and interior joints of twenty storey frame

S. No.	Joint label	Yield rotation (rad)	Yield moment (kNm)	Rotation ratio (Yield/ Ultimate)	Moment ratio (Yield/ Ultimate)
1.	IG	0.00479	1,246.14	8.36	1.36
2.	I2 - I3	0.00433	1,246.14	9.25	1.36
3.	I4 - I9	0.00473	1,229.03	8.46	1.35
4.	I10 – I15	0.00517	1,213.05	7.74	1.38
5.	I16 – I19	0.00477	932.19	8.38	1.47
6.	I20	0.00562	739.43	7.12	1.40
7.	IR	0.00784	739.43	5.10	1.27
8.	EG	8.24000	1.65	7.17	1.65
9.	E2 – E3	0.00486	1,174.34	8.24	1.65
10.	E4 – E5	0.00514	1,172.26	7.79	1.56
11.	E6 – E7	0.00553	1,169.99	7.24	1.48
12.	E – E9	0.00590	1,167.92	6.78	1.40
13.	E10 – E11	0.00634	1,166.48	6.31	1.32
14.	E12 – E13	0.00696	1,162.80	5.75	1.38
15.	E14 – E15	0.00789	1,160.15	5.07	1.35
16.	E16 – E17	0.00712	892.06	5.62	1.44
17.	E18 – E19	0.00804	890.82	4.98	1.43
18.	E20	0.00834	715.18	4.79	1.40
19.	ER	0.00853	715.18	4.69	1.31

rotation behaviour of joints. And from the moment-rotation behaviour Nonlinear Dynamic Time History Analyses of two benchmark moment frames (Tsai and Popov 1988) have been carried out. The benchmark moment frames are, two office buildings, one of six storey (Figs. 12 and 14), and other of twenty storey (Figs. 13 and 15) having peripheral MRFs, which were constructed in California, Berkeley.

Nonlinear Dynamic Time History analyses have been carried out using SAP 2000 software (CSI 2015). The earthquake ground motions considered for the analyses are 3×1952 Kern County (Taft) Earthquake for six storied frame and 1985 Mexico City Earthquake for twenty storied frame. The analyses have been carried out using the hinges obtained using proposed method as well as with standard FEMA 356 (2000) hinges. Isotropic hardening model for the hinges has been considered for the analyses purposes. The hinges properties obtained using the proposed method for both the frames have been detailed in Tables 3 and 4.

The proposed moment rotation properties have been assigned to the joints as P-M3 hinges, with zero offset from the joints, without any rigid end offsets. The proposed hinge properties incorporate the moment-rotation of beam(s) and joint panel zone, and hence does not require independent definition of panel zone element and beam hinges. The FEMA hinges have been assigned as prescribed in SAP 2000 Reference Manual. Nonlinear Dynamic Time History Analyses, for both the cases have been carried out.

Displacement time history of each of the floors of the six stored frame, using the hinges from proposed method and FEMA hinges, are compared with the published results (Tsai and Popov 1988), as shown in Figs. 16 and 17. It has been observed that the results of analysis using the proposed hinges are closely matching with the published results (Tsai and Popov 1988). Similar observations can be made from Fig. 17 which depicts the response of twenty storied building frame. It can be observed that the behaviour of frame with proposed hinges is comparatively more accurate than that with FEMA 356 hinges. The closer correspondence of results of frame with proposed hinges underlines their superiority over standard FEMA hinges.

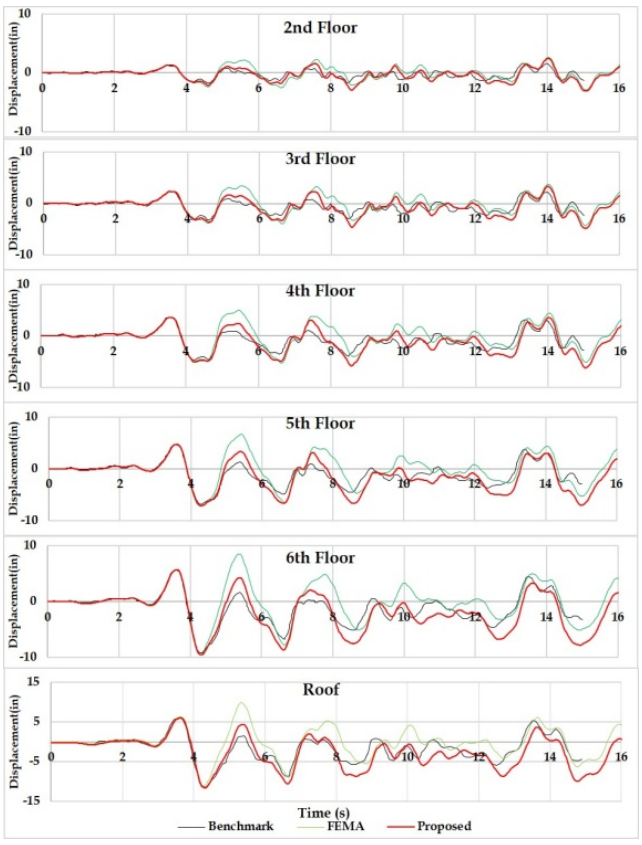

Fig. 16 Displacement response histories for all floors of the six storied frame

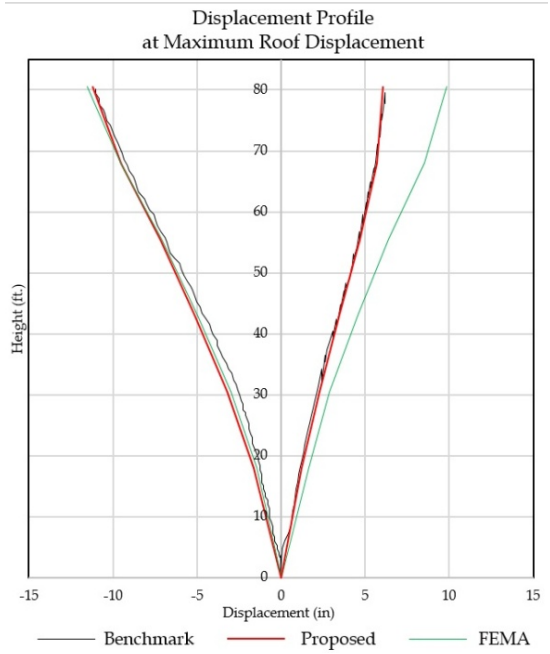

Fig. 17 Displacement profile of 20 Storied frame at maximum roof displacement

Table 5 Time required to carry out nonlinear dynamic time history analysis

Case	FEMA 356 hinges	Proposed hinges	% Reduction
6 Storied Frame (3× 1952 TAFT, N21E)	6 hours	19 minutes	94.72%
20 Storied Frame (1985 Mexico City, EW	19 hours	52 minutes	95.43%

Another key observation is that the time required to carry out the time history analyses is comparatively lesser for frames with proposed hinges than those with FEMA hinges. A comparative estimate of time required to carry out the analyses on a Intel i7 (1st generation) processor having 6GB RAM, has been presented in Table 5. This is attributed to the reduced number of points of nonlinearity from five in case of FEMA 356 hinges to three in case of proposed hinges.

4. Conclusions

A simple mechanics based hand calculation method to obtain the nonlinear force-deformation behavior of strong axis beam to column moment joints has been proposed. The approach is elegant and computationally efficient to predict the nonlinear inelastic behavior of steel MRF. The proposed method can be used to design strong and unyielding JPZ as per the design requirements. The salient features of the proposed method are summarized below:

It provides a trilinear force deformation behavior of beam to column joint subassemblages, which is applicable to both interior and exterior moment joints.

The method is able to predict the sequence of three modes of yielding - Beam Flange Yielding, Panel Zone Yielding and Formation of Plastic Hinges in beams - along with the corresponding drifts.

The proposed method can be used to obtain moment rotation characteristics for beam to column moment joints, which can be used as nonlinear hinge properties for nonlinear analysis of the frames.

The nonlinear time history analyses using proposed hinges are relatively less time consuming in comparison to that using conventional FEMA 356 hinges. This is primarily due to reduced number of points of nonlinearities at a joint. Hence the approach is very simple and computationally efficient.

References

ABAQUS (2011), ABAQUS 6.11 Analysis User's Manual; Online Documentation Help: Dassault Systèmes.

AISC 341-05 (2005), Seismic Provisions for Steel Structural Buildings; AISC 341-05, American Institute of Steel Construction, Inc., Chicago, IL, USA.

AISC 360-10 (2010), Specification for Structural Steel Buildings; AISC 360-10, American Institute of Steel Construction, Inc., Chicago, IL, USA.

Castro, J.M., Dávila-Arbona, F.J. and Elghazouli, A.Y. (2008), "Seismic design approaches for panel zones in steel moment frames", *J. Earthq. Eng.*, **12**(S1), 34-51.

Choi, S.W. and Park, H.S. (2011), "A study on the minimum column-to-beam moment ratio of steel moment resisting frame with various connection models", *Proceedings of Structures Congress*, *ASCE*.

Choi, S.W. and Park, H.S. (2012), "Multi-objective seismic design method for ensuring beam-hinging mechanism in steel frames", *J. Constr. Steel Res.*, **74**, 17-25.

Choi, S.W., Kim, Y., Lee, J., Hong, K. and Park, H.S. (2013), "Minimum column-to-beam strength ratios for beam–hinge mechanisms based on multi-objective seismic design", *J. Constr. Steel Res.*, **88**, 53-62.

CSI (2015), CSI Analysis Reference Manual for SAP2000; Computers and Structures, Inc., Berkeley, CA, USA.

Dubina, D., Ciutina, A. and Stratan, A. (2001), "Cyclic tests of double-sided beam-to-column joints", *J. Struct. Eng.*, **127**(2), 129-136.

El-Tawil, S., Vidarsson, E., Mikesell, T. and Kunnath, S.K. (1999), "Inelastic behavior and design of steel panel zones", *J. Struct. Eng.*, **125**(2), 183-193.

Engelhardt, M.D. and Sabol, T.A. (1998), "Reinforcing of steel moment connections with cover plates: Benefits and limitations", *Eng. Struct.*, **20**(4), 510-520.

FEMA-355C (2000), State of the art report on systems performance; Federal Emergency Management Agency, Washington, D.C., USA.

FEMA-356 (2000), Prestandard and commentary for the seismic rehabilitation of buildings; American Society of Civil Engineers (ASCE), Washington, D.C., USA.

Fielding, D.J. and Huang, J.S. (1971), "Shear in steel beam-to-column connections", *Welding J.*, **50**(7), 313-326.

Huang, J.S., Fielding, D. and Chen, W.F. (1972), "Future connection research problems", Fritz Laboratory Reports; Paper 296.

Jin, J. and El-Tawil, S. (2005), "Evaluation of FEMA-350 seismic provisions for steel panel zones", *J. Struct. Eng.*, **131**(2), 250-258.

Kato, B. (1982), "Cold formed welded steel tubular members",

Axially Compressed Structures, 149-180.
Krawinkler, H. (1978), "Shear in Beam-Column Joints in Seismic Design of Frames", *Eng. J.*, **15**(3).
Krawinkler, H. and Popov, E.P. (1982), "Seismic behavior of moment connections and joints", *J. Struct. Div.*, **108**(2), 373-391.
Lee, C.H., Jeon, S.W., Kim, J.H. and Uang, C.M. (2005), "Effects of panel zone strength and beam web connection method on seismic performance of reduced beam section steel moment connections", *J. Struct. Eng.*, **131**(12), 1854-1865.
Liu, X.G., Tao, M.X., Fan, J.S. and Hajjar, J.F. (2014), "Comparative study of design procedures for CFST-to-steel girder panel zone shear strength", *J. Constr. Steel Res.*, **94**, 114-121.
Mele, E., Calado, L. and De Luca, A. (2001), "Cyclic behaviour of beam-to-column welded connections", *Steel Compos. Struct., Int. J.*, **1**(3), 269-282.
Nasrabadi, M.M., Torabian, S. and Mirghaderi, S.R. (2013), "Panel zone modelling of flanged cruciform columns: An analytical and numerical approach", *Eng. Struct.*, **49**, 491-507.
Pan, L., Chen, Y., Chuan, G., Jiao, W. and Xu, T. (2016), "Experimental evaluation of the effect of vertical connecting plates on panel zone shear stability", *Thin-Wall. Struct.*, **99**, 119-131.
Popov, E.P. (1987), "Panel zone flexibility in seismic moment hoints", *J. Constr. Steel Res.*, **8**, 91-118.
Popov, E.P. (1988), "Seismic moment connections for MRFs", *J. Constr. Steel Res.*, **10**, 163-198.
Popov, E.P. and Pinkney, B.R. (1969), "Cyclic yield reversal in steel building connections", *J. Struct. Div.*
Popov, E.P., Tsai, K.C. and Engelhard, M.D. (1989) "On seismic steel joints and connections", *Eng. Struct.*, **11**(3), 148-162.
Schneider, S.P. and Amidi, A. (1998), "Seismic behavior of steel frames with deformable panel zones", *J. Struct. Eng.*, **124**(1), 35-42.
Schneider, S.P., Roeder, C.W. and Carpenter, J.E. (1993), "Seismic behavior of moment-resisting steel frames: Experimental study", *J. Struct. Eng.*, **119**(6), 1885-1902.
Tsai, K.C. and Popov, E.P. (1988), "Steel beam-column joints in seismic moment resisting frames", Report no. UCB/EERC-88/19; Earthquake Engineering Research Center, University of California, Berkeley, CA, USA.
Tuna, M. and Topkaya, C. (2015), "Panel zone deformation demands in steel moment resisting frames", *J. Constr. Steel Res.*, **110**, 65-75.
Xue, M., Kaufmann, E.J., Lu, L.W. and Fisher, J.W. (1996), "Achieving ductile behavior of moment connections - Part II", *Modem Steel Construction*.
Zekioglu, A., Mozaffarian, H. and Uang, C.M. (1997), "Moment frame connection development and testing for the city of Hope National Medical Center", *Building to Last, ASCE*.

CC

Appendix-A
Illustrative Example: Force Deformation Behaviour Using Proposed Method

The proposed method to obtain force deformation behaviour is explained for an interior beam to column strong axis joint. The joint subassemblage considered consists of column (W27×235) having a clear height of 3.8 m between supports, and two beams (W16×100) of 3 m length from column centerline. The sections selected are AISC standard sections. Column to Beam Strength Ratio for the selected beam to column joint subassemblage is 3.89.

The design constants required in the proposed method are Modulus of Elasticity (E): 200,000 MPa), Poisson's ratio (υ): 0.26 and yield strength (f_y): 250 MPa) for A36 steel. The stepwise procedure for obtaining the force deformation behaviour is given below.

I. Properties of column section

Depth of column section, $d_c = 729$ mm,
Thickness of column web, $t_{cw} = 23$ mm,
Width of column flange, $b_{cf} = 361$ mm,
Thickness of column flange, $t_{cf} = 41$ mm,

1. Check for column section class

(a) $\dfrac{b}{t_{cf}} = 4.4 < 15.83 \left(= 0.56\sqrt{\dfrac{E}{f_y}} \right)$ and

$\dfrac{h}{t_{cf}} = 28.13 < 42.14 \left(= 1.49\sqrt{\dfrac{E}{f_y}} \right)$

Thus, the section selected is a non-slender section as per AISC 361-10

2. Moment of inertia of column section

$$I_c = \left\{ \frac{b_{cf} \times d_c^3}{12} + \frac{(b_{cf} - t_{cw}) \times (d_c - 2 \cdot t_{cf})^3}{12} \right\} = 4026239063 \text{ mm}^4;$$

3. Elastic section modulus of column section

$$Z_{ec} = \frac{I_c}{(d_c / 2)} = 11045923 \text{ mm}^3;$$

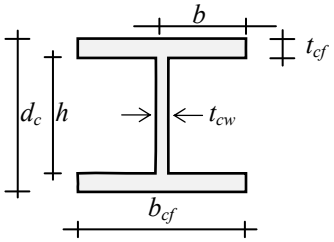

Fig. A1 Cross-section of the column

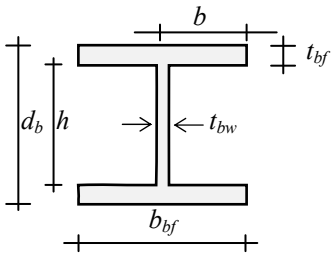

Fig. A2 Cross-section of the beam

4. Plastic section modulus of column section

$$Z_{pc} = 2\left\{ \frac{t_{cw}\left(\frac{d_c}{2} - t_{cf} \right)^2}{2} + b_{cf} t_{cf} \left(\frac{d_c}{2} - \frac{t_{cf}}{2} \right) \right\} = 11045923 \text{ mm}^3;$$

5. Shape factor for column section

$$S_c = \frac{Z_{pc}}{Z_{ec}} = 1.14;$$

6. Plastic moment capacity of column section

$$M_{pC} = \frac{f_{yc} Z_{pc}}{1000000} = 3147.52 \text{ kNm};$$

II. Properties of beam section

Depth of beam section, $d_b = 432$ mm,
Thickness of beam web, $t_{bw} = 15$ mm,
Width of column flange, $b_{bf} = 264$ mm,
Thickness of column flange, $t_{bf} = 25$ mm,

7. Check for beam section class

(a) $\dfrac{b}{t_{cf}} = 5.28 < 10.75 \left(= 0.38\sqrt{\dfrac{E}{f_y}} \right)$ and

$\dfrac{h}{t_{vw}} = 25.47 < 106.35 \left(= 3.76\sqrt{\dfrac{E}{f_y}} \right)$

Thus, the section selected is a compact section as per AISC 361-10.

8. Moment of inertia of column section

$$I_b = \left\{ \frac{b_{bf} \times d_b^3}{12} + \frac{(b_{bf} - t_{bw}) \times (d_b - 2 \cdot t_{bf})^3}{12} \right\} = 617007910 \text{ mm}^4;$$

9. Elastic section modulus of column section

$$Z_{eb} = \frac{I_b}{(d_b / 2)} = 2856518 \text{ mm}^3;$$

10. Plastic section modulus of column section

$$Z_{pb} = 2\left\{\frac{t_{bw}\left(\frac{d_b}{2} - t_{bf}\right)^2}{2} + b_{bf}t_{cb}\left(\frac{d_b}{2} - \frac{t_{bf}}{2}\right)\right\} = 3233415\ \text{mm}^3;$$

11. Shape factor for column section

$$S_b = \frac{Z_{pb}}{Z_{eb}} = 1.132;$$

12. Plastic moment capacity of column section

$$M_{pB} = \frac{f_{yb}Z_{pb}}{1000000} = 808.35\ \text{kNm}.$$

Thus, the Column to Beam Strength Ratio (CBSR) for selected interior joint subassemblage is $CBSR = \frac{2 \times M_{pC}}{2 \times M_{pB}}$ $= 3.89$.

13. If doubler plates are provided, the thickness of column web at the JPZ level increases. This increased thickness of JPZ is taken into consideration as, $t_{pz} = (t_{cw} + t_{dp})$ where t_{dp} is the total thickness of doubler plates provided.

III. Yielding modes and sequence

For Interior beam to column joint subassemblages,

14. Beam flange yield strength

$$F_{y,bf} < \frac{f_y \times b_{bf} \times t_{bf}}{1000} = 1650\ \text{kN}$$

15. Panel zone yield strength

$$V_{y,pz} = \left(\frac{f_y}{\sqrt{3}} \times d_c \times t_{pz}\right) \Big/ 1000 = 2420\ \text{kN}$$

16. Beam Flange force, corresponding to plastic flexural strength of beam, M_{pB}

$$F_{p,bf} = \frac{M_{pB}}{(d_b - t_{bf}) \times 1000} = 1986.13\ \text{kN}$$

Since, $V_{u,pz} < 2 \times F_{y,bf} < 2 \times F_{p,bf}$, the yielding sequence will be

(a) JPZ Yielding,
(b) Beam Flange Yielding,
(c) Beam Plastic Hinge formation

IV. Yield forces

17. Shear force in beam corresponding to its plastic flexural strength is

$$V_{pB} = \frac{M_{pB}}{\left(\frac{L_b - d_c}{2}\right) \times 1000} = 306.72\ \text{kN}$$

18. Beam end force required for shear yielding of JPZ (P)

$$V_{y1} = \left(\frac{V_{y,pz}}{2}\right) \times \left(\frac{d_b - t_{cf}}{L_b/2 - d_c/2}\right) = 186.87\ \text{kN}$$

19. Beam end force for beam flange yielding (BFY)

$$V_{y2} = \frac{F_{y,bf}(d_b - t_{bf})}{(L_b/2 - d_c/2)} = 254.81\ \text{kN}$$

20. Beam end force for formation of plastic hinge in beams (BPH)

$$V_{y3} = \frac{F_{p,bf}(d_b - t_{bf})}{(L_b/2 - d_c/2)} = 306.72\ \text{kN}$$

21. Beam stiffness

(a) Post- first (flange) yielding:

$$K_{b1} = \frac{\left(\frac{1}{12} \times t_{bw} \times d_b^3\right)}{I_b} = 0.16$$

(b) Post formation of plastic hinges:
$K_{b2} = 0.05$ (Assumed)

V. Post-yield stiffnesses

22. Panel zone stiffness

(a) Immediately following yield:
$K_{pz1} = 0.07$ (Literature (Krawinkler 1978))
(b) Post significant yield:
$K_{pz2} = 0.03$ (Literature (Krawinkler 1978))

VI. First yield event

At the initiation of first yield

23. Beam end force

$$V_{y1} = \frac{V_{y,pz}}{2} \times \frac{(d_b - t_{bf})}{(L_b/2 - d_c/2)} = 186.87\ \text{kN}$$

24. Bending moment in column

$$M_{c1} = \frac{2 \times V_{y1} \times (L_b/2)}{1000} = 1121.21\ \text{kNm}$$

25. Rotation of columns

$$\theta_{c1} = \frac{(M_{c1}/2)\times 1000000\times(L_b/2)}{3\times E\times I_c} = 0.00044092\,\text{rad}$$

26. Shear in JPZ

$$V_{pz,1} = \frac{2\times V_{y1}\times(L_b/2-d_c/2)}{(d_b-t_{bf})} = 2420.11\,\text{kN}$$

27. JPZ deformation

$$\gamma_{pz1} = \frac{V_{pz,1}\times 1000}{G\times d_c\times t_{pz}} = 0.00181865\,\text{rad}$$

28. Drift in column

$$\Delta_{c1} = \theta_{c1} = \frac{L_b}{2} = 1.323\,\text{mm}$$

29. Drift in JPZ

$$\Delta_{pz1} = \gamma_{pz1}\times(L_b/2-d_c/2) = 4.793\,\text{mm}$$

30. Drift in beam

$$\Delta_{b1} = \frac{V_{y1}\times 1000\times(L_b/2-d_c/2)^3}{3\times E\times I_b} = 9.240\,\text{mm}$$

31. Total drift at first yield

$$\Delta_{total1} = \Delta_{c1}+\Delta_{pz1}+\Delta_{b1} = 15.356\,\text{mm}$$

32. Percentage drift at first yield

$$\%D_1 = \frac{\Delta_{total1}}{L_b/2}\times 100 = 0.512\%$$

VII. Second yield event

Post first yield

33. Beam end force

$$V_{y2} = \frac{F_{y,bf}(d_b-t_{bf})}{(L_b/2-d_c/2)} = 254.81\,\text{kN}$$

34. Bending moment in column

$$M_{c2} = \frac{2\times V_{y2}\times(L_b/2)}{1000} = 1528.86\,\text{kNm}$$

35. Rotation of columns

$$\theta_{c2} = \frac{(M_{c2}/2)\times 1000000\times(L_c/2)}{3\times E\times I_c} = 0.00060123\,\text{rad}$$

36. Shear in JPZ

$$V_{pz,2} = \frac{2\times V_{y2}\times(L_b/2-d_c/2)}{(d_b-t_{bf})} = 3300\,\text{kN}$$

37. JPZ deformation

$$\gamma_{pz2} = \gamma_{pz1}+\frac{(V_{pz,2}-V_{pz,1})\times 1000}{(0.07\times G)\times d_c\times t_{pz}} = 0.0112646\,\text{rad}$$

38. Drift in column

$$\Delta_{c2} = \theta_{c2} = \frac{L_b}{2} = 1.804\,\text{mm}$$

39. Drift in JPZ

$$\Delta_{pz2} = \gamma_{pz2}\times(L_b/2-d_c/2) = 29.688\,\text{mm}$$

40. Drift in beam

$$\Delta_{b2} = \frac{V_{y2}\times 1000\times(L_b/2-d_c/2)^3}{3\times E\times I_b} = 12.600\,\text{mm}$$

41. Total drift at first yield

$$\Delta_{total2} = \Delta_{c2}+\Delta_{pz2}+\Delta_{b2} = 44.091\,\text{mm}$$

42. Percentage drift at first yield

$$\%D_1 = \frac{\Delta_{total2}}{L_b/2}\times 100 = 1.47\%$$

VIII. Third yield event

At initiation of third yield event

43. Beam end force

$$V_{y3} = \frac{F_{p,bf}(d_b-t_{bf})}{(L_b/2-d_c/2)} = 306.72\,\text{kN}$$

44. Bending moment in column

$$M_{c3} = \frac{2\times V_{y3}\times(L_b/2)}{1000} = 1840.3\,\text{kNm}$$

45. Rotation of columns

$$\theta_{c3} = \frac{(M_{c3}/2)\times 1000000\times(L_c/2)}{3\times E\times I_c} = 0.0007237\,\text{rad}$$

46. Shear in JPZ

$$V_{pz,3} = \frac{2\times V_{y3}\times(L_b/2-d_c/2)}{(d_b-t_{bf})} = 3972.25\,\text{kN}$$

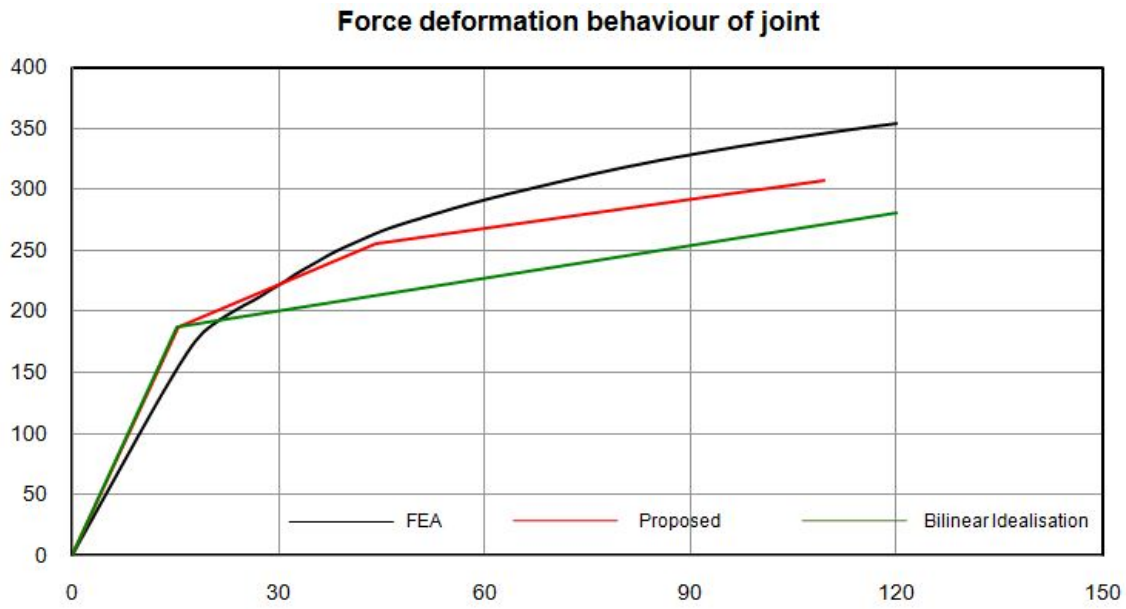

Fig. A3 Force Deformation Behaviour of an interior beam to column joint subassemblage

47. JPZ deformation

$$\gamma_{pz3} = \gamma_{pz2} + \frac{(V_{pz,3} - V_{pz,2}) \times 1000}{(0.03 \times G) \times d_c \times t_{pz}} = 0.028104 \text{ rad}$$

48. Drift in column

$$\Delta_{c3} = \theta_{c3} = \frac{L_b}{2} = 2.171 \text{ mm}$$

49. Drift in JPZ

$$\Delta_{pz3} = \gamma_{pz3} \times (L_b / 2 - d_c / 2) = 74.068 \text{ mm}$$

50. Drift in beam

$$\Delta_{b3} = \Delta_{b2} + \frac{(V_{y3} - V_{y2}) \times 1000 \times (L_b / 2 - d_c / 2)^3}{(3 \times E \times I_b) \times 0.16} = 28.315 \text{ mm}$$

51. Total drift at first yield

$$\Delta_{total3} = \Delta_{c3} + \Delta_{pz3} + \Delta_{b3} = 104.554 \text{ mm}$$

52. Percentage drift at first yield

$$\%D_1 = \frac{\Delta_{total3}}{L_b / 2} \times 100 = 3.485\%$$

IX. Bilinear idealization

This method provides a tri-linear curve, representing the force deformation behaviour of the beam to column joint considered for this illustration (Fig. A1). To utilize this proposed curve for Nonlinear Dynamic Time History Analysis of frames, a bilinear idealization of the force deformation behaviour is required. The method of idealization adopted for the present study is presented in this section.

53. Beam end force at first yield

$$V_{y1} = 186.67 \text{ kN}$$

54. Total drift at first yield

$$\Delta_{total1} = 15.356 \text{ mm}$$

55. Average of second and third yield forces

$$V'_{y2} = \frac{V_{y2} + V_{y3}}{2} = 280.77 \text{ kN}$$

56. Target drift required

$$\Delta_t = 120 \text{ mm}$$